Cellular/Molecular

# A JIP3-Regulated GSK3β/DCX Signaling Pathway Restricts Axon Branching

**Parizad M. Bilimoria,[1,2] Luis de la Torre-Ubieta,[1,2] Yoshiho Ikeuchi,[1] Esther B. E. Becker,[1] Orly Reiner,[3] and Azad Bonni[1,2]**

[1]Department of Pathology and [2]Program in Neuroscience, Harvard Medical School, Boston, Massachusetts 02115, and [3]Department of Molecular Genetics, The Weizmann Institute of Science, Rehovot 76100, Israel

**Axon branching plays a critical role in establishing the accurate patterning of neuronal circuits in the brain. However, the mechanisms that control axon branching remain poorly understood. Here we report that knockdown of the brain-enriched signaling protein JNK-interacting protein 3 (JIP3) triggers exuberant axon branching and self-contact in primary granule neurons of the rat cerebellar cortex. JIP3 knockdown in cerebellar slices and in postnatal rat pups *in vivo* leads to the formation of ectopic branches in granule neuron parallel fiber axons in the cerebellar cortex. We also find that JIP3 restriction of axon branching is mediated by the protein kinase glycogen synthase kinase 3β (GSK3β). JIP3 knockdown induces the downregulation of GSK3β in neurons, and GSK3β knockdown phenocopies the effect of JIP3 knockdown on axon branching and self-contact. Finally, we establish doublecortin (DCX) as a novel substrate of GSK3β in the control of axon branching and self-contact. GSK3β phosphorylates DCX at the distinct site of Ser327 and thereby contributes to DCX function in the restriction of axon branching. Together, our data define a JIP3-regulated GSK3β/DCX signaling pathway that restricts axon branching in the mammalian brain. These findings may have important implications for our understanding of neuronal circuitry during development, as well as the pathogenesis of neurodevelopmental disorders of cognition.**

## Introduction

The branching pattern of an axon defines the spatial distribution of its outputs, specifying the landscape for potential sites of connectivity with postsynaptic partners. Axon branching both establishes general targets of innervation and sculpts on a finer scale the field of innervation within a specific target. The restriction of axon branches to appropriate locales is critical for normal neuronal connectivity and is accomplished by regulating the formation and patterning of branches. A key feature of axon branch patterning is self-avoidance, which represents the restriction in overlap of branches within the same neuron. The functional consequences of axon branch number and placement for neural circuits underscores the importance of elucidating the mechanisms that regulate axon branching in the brain.

While the regulation of axon growth has been the subject of intense investigation, much less is known about the molecular control of axon branching. Although a few molecules implicated in axon growth have been found to also modulate axon branching (Kornack and Giger, 2005), the signaling mechanisms that control axon branching in the mammalian brain remain primarily to be elucidated. Furthermore, the molecular control of self-avoidance of axon branches is poorly understood.

The JNK-interacting proteins (JIPs) comprise a family of signaling proteins first identified for their role in organizing c-Jun N-terminal kinase (JNK) signaling cascades (Whitmarsh and Davis, 1998; Ito et al., 1999; Yasuda et al., 1999; Kelkar et al., 2000). Among the JIPs, JIP3 is selectively enriched in the brain (Kelkar et al., 2000; Akechi et al., 2001). The expression of JIP3 is high in axon bundles in the developing rodent brain (Akechi et al., 2001). Consistent with these observations, JIP3 appears to be enriched within the growth cone in neuronal processes (Verhey et al., 2001; Sato et al., 2004). The JIP3 orthologs in *Drosophila* and *Caenorhabditis elegans*, Sunday Driver and UNC-16, respectively, operate as adaptors for the motor protein kinesin and thereby regulate vesicular transport (Bowman et al., 2000; Byrd et al., 2001). In other studies, the protein kinase JNK has been implicated in the specification of axons in primary hippocampal neurons and in maintaining the integrity of cortical axon tracts *in vivo* (Chang et al., 2003; Oliva et al., 2006). Together, these studies raised the question of whether JIP3 might regulate axon development. Whether and how JIP3 plays a role in axon branching morphogenesis remained unknown.

In this study, we identify a cell-autonomous function for JIP3 in axon branching morphogenesis. Knockdown of JIP3 stimulates axon branching in primary granule neurons and in the rat cerebellar cortex *in vivo*. Remarkably, the ectopic axon branches in JIP3 knockdown neurons fail to avoid self-contact. Surprisingly, JIP3 appears to inhibit axon branching and self-contact in a JNK-independent manner. Rather, we find that JIP3 regulates axon branching and self-contact via the protein kinase glycogen

Received March 16, 2010; revised June 21, 2010; accepted June 27, 2010.

This work was supported by National Institutes of Health Grants NS041021 and NS047188 (A.B.). We thank Katsuji Yoshioka for the pmMKO.1/JIP3i plasmid, Kristen Verhey for the pU6-puro/JIP3i plasmid, Gaëlle Friocourt for the psiStrike/DCXi and pCAG/DCX–IRES–GFP plasmids, Jonathon Kurie for the pSuper/JNK1,2i plasmid, and Joan Brugge for the HA–FAK plasmid. We thank Gabriel Corfas, Wade Harper, Bernardo Sabatini, and members of the Bonni laboratory for helpful discussions and critical reading of this manuscript.

Correspondence should be addressed to Azad Bonni, Department of Pathology, Harvard Medical School, 77 Avenue Louis Pasteur, New Research Building, Room 856, Boston, MA 02115. E-mail: azad_bonni@hms.harvard.edu.

DOI:10.1523/JNEUROSCI.1362-10.2010

 0270-6474/10/3016766-11$15.00/0

synthase kinase 3β (GSK3β). We also uncover the X-linked lissencephaly protein doublecortin (DCX) as a novel substrate of GSK3β. GSK3β induces the phosphorylation of DCX at Ser327, which contributes to DCX function in the inhibition of axon branching and self-contact. These findings define a novel JIP3-regulated GSK3β/DCX signaling pathway that restricts axon branching, thus providing important insights into our understanding of axon branch patterning in the mammalian brain. In addition, because DCX mutations are a cause of inherited mental retardation and epilepsy (Allen and Walsh, 1999), our findings suggest that deregulation of the JIP3-controlled GSK3β/DCX signaling pathway and axon branching may contribute to the pathogenesis of neurodevelopmental disorders of cognition.

## Materials and Methods

*Plasmids.* RNA interference (RNAi) plasmids all encode short hairpin RNAs (shRNAs) under control of the U6 RNA polymerase III promoter. The U6/JIP3i, U6/GSK3βi1, U6/GSK3βi2, U6/FAKi1, and U6/FAKi2 RNAi plasmids were generated by cloning the following oligonucleotides into a pBluescript vector containing the U6 promoter, with the underlined portion representing the target sequence: U6/JIP3i, 5′-CACCGTGATGCTGTCAAATTATTCAAGCTTGAATTTGACAGCATCACGGTGCTTTTTTTG-3′ (this sequence is preceded by a G in the vector that is also part of the target sequence); U6/GSK3βi1, 5′-ACATTAAACCACAGAACCTCTTTCGTTAACTGAGGTTCTGTGGTTTAATGTCTTTTTG-3′; U6/GSK3βi2, 5′- ACTCAAGAACTGTCAAGTAACTTCGTTAACCTTACTTGACAGTTCTTGAGTCTTTTTG-3′; U6/FAKi1, 5′- GATCCAATGACAAGGTATATGTTCGTTAACGATATACCTTGTCATTGGATCCTTTTTG-3′; U6/FAKi2, 5′- GCCAACCTTAATAGAGAAGATTCGTTAACACTTCTCTATTAAGGTTGGCACTTTTTG-3′.

The RNAi-resistant FLAG–JIP3–RES expression plasmid was generated using site-directed mutagenesis to introduce silent mutations in JIP3. Mutations of the RNAi target sequence are denoted by lowercase letters: 5′-G CAt aga GAT GCT GTC AAA TTC T-3′.

The pmMKO.1/JIP3i and the pU6-puro/JIP3i RNAi plasmids have been described previously (Bayarsaikhan et al., 2007; Hammond et al., 2008). The DCX RNAi plasmid (psiStrike/DCXi), targeting the 3′ untranslated region sequence of DCX, and the corresponding control plasmid (psiStrike/Ctrl), containing 3 bp mutations to the DCX hairpin sequence, are described, as is the pCAG/DCX–internal ribosomal entry site (IRES)–green fluorescent protein (GFP) expression plasmid (Bai et al., 2003; Friocourt et al., 2007). FLAG–DCX/pCDNA3 and glutathione *S*-transferase (GST)–DCX/pGEX plasmids have also been described previously (Gdalyahu et al., 2004).

*Primary granule neurons.* Cultures of cerebellar granule neurons were prepared from postnatal day 6 (P6) rats as described previously (Bilimoria and Bonni, 2008). For morphology experiments, neurons were transfected by the calcium phosphate method within 1 d of plating and fixed 4 d later. To diminish the possibility that any of the morphological phenotypes observed with our constructs of interest were attributable to effects of these constructs on neuronal survival, we included an expression plasmid for the antiapoptotic protein gene Bcl-xL, which has been shown to have little or no effect on dendritic or axonal morphology in granule neurons (Gaudillière et al., 2004; Konishi et al., 2004). For biochemistry experiments, neurons were electroporated before plating using the Amaxa nucleofection system and lysed 4–6 d later.

*Immunocytochemistry.* Granule neurons were fixed in 4% paraformaldehyde, permeabilized with 0.4% Triton X-100, and then immunostained using the rabbit anti-GFP (Invitrogen), mouse anti-GFP (NeuroMab), rabbit anti-Discosoma red (DsRed, Clontech), mouse anti-Tuj1 (Covance), mouse anti-MAP2 (Sigma), rabbit anti-JIP3 (Santa Cruz Biotechnology), rabbit anti-DCX (Cell Signaling Technology), or mouse anti-GSK3β (BD Biosciences) antibody. Nuclei were labeled with the DNA dye bisbenzimide (Hoechst 33258).

*Morphological analysis.* Images were captured on an epifluorescence microscope and analyzed in a blinded manner using Spot Advanced software (Diagnostic Instruments). Axon tips were defined as terminal points of the primary axon and all of its branches. Self-contact points were defined as any instance in which the primary axon or one of its branches appeared to touch or cross over either itself or any other portion of the axon. Confocal analyses established that points of self-contact observed in the two-dimensional images used for measurements were also detected in single optical sections of three-dimensional image series acquired in 0.4 μm step intervals on a 60× objective (data not shown). Primary axon length was measured by tracing the axonal fiber emanating from the soma in a manner that produced the longest continuous path.

*Time-lapse imaging.* Granule neurons were plated on Lab-Tek II glass-bottom chambers (Thermo Fisher Scientific Nunc). Live imaging was performed using a Nikon Ti-E Perfect-Focus microscope equipped with a PerkinElmer Life and Analytical Sciences UltraVIEW spinning-disk confocal system. An environment-controlled chamber maintained the neurons at 37°C, 5% $CO_2$. Images were acquired and analyzed using Volocity software (PerkinElmer Life and Analytical Sciences). A 20× objective was used in combination with an automated stage to capture images every 15 min for a period of 1–2 d, starting 24 h after transfection. Neurons were chosen randomly, and, at the start of image acquisition, the axon terminus was positioned at the center of the field.

*Organotypic cerebellar slices.* Organotypic cerebellar slices were prepared from postnatal day 10 rat pups as described previously (Gaudillière et al., 2004). Briefly, a tissue chopper was used to cut 400 μm sagittal slices, which were maintained on a porous membrane (Millicell) that allows for an air–media interface. Slices were transfected using the Helios gene gun system (Bio-Rad) at day *in vitro* 4 (DIV4) and fixed at DIV8 in 4% paraformaldehyde and subjected to immunohistochemistry.

In vivo *electroporation.* P3 rat pups were electroporated as described previously (Konishi et al., 2004). Animals were killed 5 d after electroporation. Cerebella were fixed in 4% paraformaldehyde, sunk in a 30% sucrose solution, and subsequently frozen in Tissue Tek OCT compound. Cryostat sections were cut coronally at 30 μm and immunostained with the GFP antibody. Layers of the cerebellar cortex were identified by staining nuclei with Hoechst.

*Real-time reverse transcription-PCR.* RNA was extracted from granule neurons using the TRIzol reagent (Invitrogen). The SuperScript III First-Strand Synthesis System (Invitrogen) for reverse transcription (RT)-PCR was used to prepare cDNA from the extracted RNA. The reverse transcription reaction was conducted at 50°C for 50 min. Real-time PCR was subsequently performed using the LightCycler 480 SYBR Green I Master kit (Roche). The PCR reaction consisted of an initial 95°C incubation for 10 min, followed by 40 cycles of the following sequence: 95°C for 10 s, 60°C for 20 s, and 72°C for 30 s, then acquisition of melting curves and cooling. Primer sequences were as follows: glyceraldehyde-3-phosphate dehydrogenase (GAPDH), forward, 5′-TGCTGGTGCTGAGTATGTCG-3′ and reverse, 5′-GCATGTCAGATCCACAACGG-3′; JIP3, forward, 5′-TGCCTTGGAACAAGAGAAGAAAG-3′ and reverse, 5′-CCACATAGGTCTGGATCATCTCC-3′; and GSK3β, forward, 5′-CAAGCAGACACTCCCTGTGA-3′ and reverse, 5′-GTGGCTCCAAAGATCAGCTC-3′.

*Immunoblotting.* Human embryonic kidney HEK293T cells and neurons were both lysed in 50 mM Tris, pH 7.5, 150 mM NaCl, 2 mM EDTA, and 1% Triton X-100. The protease inhibitors aprotinin, pepstatin, leupeptin, and phenylmethanesulfonyl fluoride, the phosphatase inhibitors sodium fluoride, β-glycerolphosphate, sodium orthovanadate, and okadaic acid, as well as the reducing agent dithiothreitol were added to this buffer before cell lysis. Lysates were cleared of insoluble material by spinning at maximum speed on a tabletop centrifuge, boiled in sample buffer, and examined using standard SDS-PAGE, followed by Western blotting. The antibodies used were rabbit anti-JIP3 (Santa Cruz Biotechnology), rabbit anti-GFP (Invitrogen), mouse anti-FLAG (Sigma), mouse anti-HSP60 (Santa Cruz Biotechnology), mouse anti-GSK3 (Assay Designs), rabbit polyclonal anti-DCX (Cell Signaling Technology), mouse anti-14-3-3β (Santa Cruz Biotechnology), mouse anti-hemagglutinin (HA) (Roche), rabbit anti-SnoN (Santa Cruz Biotechnology), and rabbit anti-JNK1 (Santa Cruz Biotechnology). The rabbit anti-phospho-DCX Thr321, Ser327 antibody has been described previously (Gdalyahu et al., 2004). The following pharmacological agents were used: 6′bro-

moindirubin-3′-oxime (also known as BIO) (Calbiochem), MG132 (carbobenzoxy-L-leucyl-L-leucyl-L-leucinal) (Sigma), and SP600125 (anthra[1,9-cd]pyrazol-6(2*H*)-one) (Sigma).

In vitro *kinase assay.* Kinase assays examining the phosphorylation of bacterially produced GST–DCX by GSK3$\beta$ (New England Biolabs) were performed sequentially. The GST–DCX substrates, bound to glutathione Sepharose beads, were first primed in a kinase reaction with FLAG–JNK1 purified from HEK293T cells, then washed with high salt to remove the JNK, and finally subjected to a GSK3$\beta$ kinase assay using [$\gamma$-$^{32}$P]ATP. The JNK reaction was performed under the following conditions (in mM): 20 HEPES, pH 7.4, 20 $MgCl_2$, 1 dithiothreitol, 0.1 sodium orthovanadate, 100 $\beta$-glycerolphosphate, and 10 nonradiolabeled ATP (for 3 h at 30°C). The GSK3$\beta$ reaction was performed under the following conditions: 20 mM Tris-HCl, 10 mM $MgCl_2$, 5 mM dithithreitol, 200 $\mu$M nonradiolabeled ATP, and 10 $\mu$Ci [$\gamma$-$^{32}$P]ATP, for 30 min at 30°C. Approximately 500 ng of substrate was incubated with 250 U of the GSK3$\beta$ kinase.

The FLAG–JNK1 purified from HEK293T cells was activated by UV irradiation 30 min before lysis. Lysates were subjected to immunoprecipitation using agarose beads conjugated to the FLAG antibody (Sigma), washed in high salt, and eluted with 3× FLAG peptide (Sigma).

*Statistics.* Statistical analyses were performed using Statview and Excel software. Error bars on bar graphs denote SEM. The *t* test was used to evaluate significance of comparisons in experiments with only two groups. ANOVA was performed followed by Fisher's *post hoc* least significant difference (PLSD) test for pairwise comparisons in experiments with more than two groups. Except when indicated otherwise, asterisks on bar graphs denote statistical significance in comparisons with the control condition: $^{*}p < 0.05$, $^{**}p < 0.01$, and $^{***}p < 0.001$.

## Results

### JIP3 restricts axon branching in cerebellar granule neurons

To investigate the role of the signaling protein JIP3 in axon morphogenesis, we characterized JIP3 function in granule neurons of the cerebellar cortex. Granule neurons represent a robust model system for elucidation of the molecular underpinnings of neuronal morphogenesis (Altman and Bayer, 1997; Hatten, 1999). Granule neuron precursors differentiate into postmitotic neurons within the external granule layer (EGL). Newly generated granule neurons extend axons that continue to grow as the granule neuron somas descend into the internal granule layer (IGL). Granule neuron axons form characteristic T-shaped structures, composed of an ascending axon and two major parallel fiber branches that run in the molecular layer (ML) along the coronal plane of the cerebellar cortex, in which they participate in en passant synapses with Purkinje neuron dendrites (Ramon y Cajal, 1995; Altman and Bayer, 1997). Typically, parallel fiber axons give rise to at most one more branch in the ML (Ramon y Cajal, 1995). The morphological characteristics of granule neuron axons make these neurons ideal for unraveling the mechanisms that restrict axon branching.

To determine JIP3 function in neuronal morphogenesis, we used a plasmid-based method of RNAi to acutely knockdown JIP3 (Gaudillière et al., 2002). Expression of shRNAs targeting JIP3 (U6/JIP3i) substantially reduced the levels of both exogenous JIP3 in heterologous cells and endogenous JIP3 in granule neurons (Fig. 1*A*). We transfected granule neurons with the U6/JIP3i RNAi or control U6 plasmid together with a GFP expression plasmid, the latter to visualize granule neuron morphology. Axons and dendrites of granule neurons are easily identified based on their characteristic morphological features and expression of axon- or dendrite-specific markers (Gaudillière et al., 2004; Konishi et al., 2004). Control primary granule neurons transfected with the control U6 plasmid harbored characteristic morphological features of granule neurons in the cerebellar cortex, including multiple short, branched dendrites and long axons bearing few or no branches (Fig. 1*B*). Strikingly, we found that JIP3 knockdown triggered exuberant branching of axons in granule neurons (Fig. 1*B*). Axons in JIP3 knockdown granule neurons had excessive branches, which were often in the distal portions of the axon (Fig. 1*B*). The JIP3 knockdown-induced branching in the distal axon correlated with the spatial pattern of JIP3 expression in granule neurons. Both exogenous GFP–JIP3 and endogenous JIP3 were enriched in the distal portion of the axon in granule neurons (supplemental Fig. S1*A*,*B*, available at www.jneurosci.org as supplemental material). Remarkably, axon branches in JIP3 knockdown neurons also failed to avoid self-contact compared with axon branches in control granule neurons (Fig. 1*B*). Quantification revealed an approximately threefold increase in the number of axonal tips in JIP3 knockdown granule neurons compared with control U6-transfected neurons (Fig. 1*C*). In addition, JIP3 knockdown increased by fivefold the number of axon self-contact events in granule neurons (Fig. 1*C*). In other analyses, we found that JIP3 knockdown led to reduction in axon length (supplemental Fig. S2*A*, available at www.jneurosci.org as supplemental material), suggesting the JIP3 RNAi-induced phenotype of increased axon branching is not attributable to a general increase in axon growth. We also found that JIP3 RNAi had little or no effect on dendrite length in granule neurons (supplemental Fig. S2*B*, available at www.jneurosci.org as supplemental material). Collectively, our data suggest that JIP3 knockdown stimulates axon branching and self-contact in neurons.

To confirm that the JIP3 RNAi-induced axon branching and self-contact phenotype is attributable to specific knockdown of JIP3 rather than off-target effects of JIP3 shRNAs or nonspecific activity of the RNAi machinery, we performed a rescue experiment. We designed an expression plasmid encoding an RNAi-resistant rescue form of the JIP3 (JIP3–RES). JIP3 RNAi induced knockdown of FLAG–JIP3 encoded by wild-type cDNA (WT) but failed to effectively induce knockdown of FLAG–JIP3–RES in cells (Fig. 1*D*). In morphology assays, expression of FLAG–JIP3–RES reversed the JIP3 RNAi-induced phenotypes of axon branching and self-contact (Fig. 1*E*,*F*). These results suggest that the JIP3 RNAi-induced axon branching phenotype is the result of specific knockdown of JIP3 in granule neurons. Further corroborating these data, knockdown of JIP3 by two additional shRNAs targeting distinct regions of JIP3 robustly induced axon branching and increased axon self-contact, thus mimicking the effect of shRNAs encoded by the U6/JIP3 RNAi plasmid (Fig. 1*G*,*H*) (supplemental Fig. S3*A–C*, available at www.jneurosci.org as supplemental material). Collectively, our data suggest that JIP3 plays a specific and essential role in the suppression of axon branching and may promote axon self-avoidance.

### JIP3 suppresses axon branching in the cerebellar cortex *in vivo*

Having established that endogenous JIP3 inhibits axon branching in primary granule neurons, we next determined the cell-autonomous function of JIP3 in the context of the intact cerebellar cortex. We first assessed the effect of JIP3 knockdown in organotypic cerebellar slices (Fig. 2*A*). Using a biolistics approach, we transfected cerebellar slices from P9 rat pups with the U6/JIP3i RNAi or control U6 plasmid together with the GFP expression plasmid. After 4 d, cerebellar slices were subjected to immunohistochemistry using the GFP antibody. Granule neurons in the IGL were analyzed. Granule neurons in cerebellar slices transfected with the control U6 plasmid harbored normal

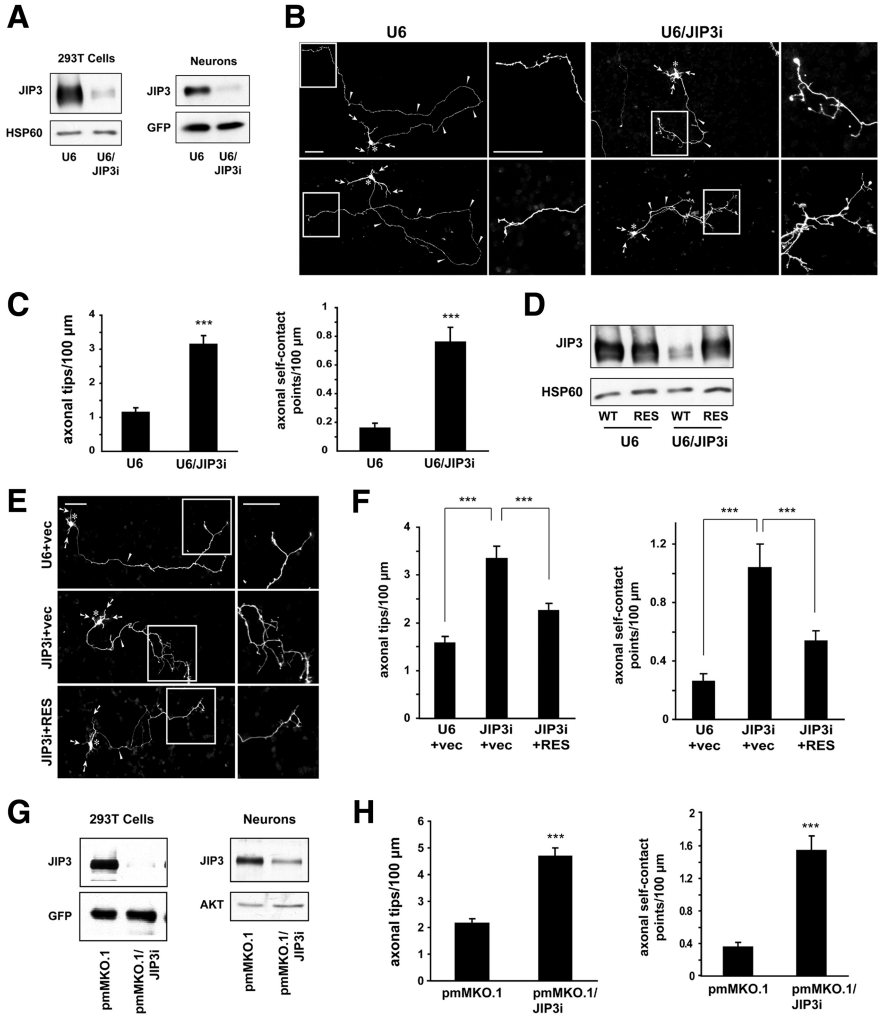


**Figure 1.** JIP3 restricts axon branching in cerebellar granule neurons. ***A***, Left, Lysates of HEK293T cells transfected with the FLAG–JIP3 expression plasmid and the U6/JIP3i or control U6 RNAi plasmid were immunoblotted with the FLAG and HSP60 antibodies, the latter serving as a loading control. Right, Lysates of granule neurons nucleofected with the U6/JIP3i or control U6 RNAi plasmid together with a GFP expression plasmid were immunoblotted using the JIP3 and GFP antibodies, the latter serving as a control for loading and transfection efficiency. ***B***, Granule neurons transfected with the U6/JIP3i or control U6 RNAi plasmid together with the GFP expression plasmid were fixed 4 d after transfection and subjected to immunocytochemistry using the GFP antibody. For each representative image, boxed regions in the left panel highlight the distal axon, which is shown at higher magnification in the right panel. In all images of this type, arrows indicate dendrites, asterisks the soma, and arrowheads the axon. Scale bars, 50 $\mu$m. JIP3 knockdown triggered the formation of exuberant axon branches. ***C***, Quantification of axon branching of granule neurons treated as in ***B***. JIP3 knockdown significantly increased the number of axonal tips per hundred micrometers (*t* test, $p < 0.001$) and the number of axonal self-contact points per hundred micrometers (*t* test, $p < 0.001$). A total of 160 neurons were measured. Error bars here and in all subsequent bar graphs denote + SEM. Except when indicated otherwise, in all figures asterisks on bar graphs denote statistical significance compared with the control condition: $^{*}p < 0.05$, $^{**}p < 0.01$, and $^{***}p < 0.001$. ***D***, Lysates of HEK293T cells transfected with FLAG–JIP3 encoded by wild-type cDNA (WT) or an RNAi-resistant cDNA (RES) and the U6/JIP3i or control U6 RNAi plasmid were immunoblotted using the FLAG and HSP60 antibodies. JIP3 knockdown decreased levels of FLAG–JIP3 but not FLAG–JIP3–RES. ***E***, Granule neurons transfected with the FLAG–JIP3–RES or control vector expression plasmid and the U6/JIP3i or control U6 RNAi plasmid together with the GFP expression plasmid were analyzed as in ***B***. Scale bars, 50 $\mu$m. ***F***, Quantification of axon branching of granule neurons treated as in ***E***. In the vector background, JIP3 knockdown significantly increased the number of axonal tips per hundred micrometers (ANOVA followed by Fisher's PLSD test, $p < 0.001$) and the number of axonal self-contact points per hundred micrometers (ANOVA followed by Fisher's PLSD test, $p < 0.001$). In the background of JIP3 knockdown, expression of FLAG–JIP3–RES, compared with the corresponding vector, significantly decreased the number of axonal tips per hundred micrometers (ANOVA followed by Fisher's PLSD test, $p < 0.001$) and the number of axonal self-contact points per hundred micrometers (ANOVA followed by Fisher's PLSD test, $p < 0.001$). A total of 225 neurons were measured. ***G***, Left, Lysates of HEK293T cells transfected with the FLAG–JIP3 expression plasmid and the pmMKO.1/JIP3i or control pmMKO.1 RNAi plasmid were immunoblotted using the FLAG and GFP antibodies. Right, Lysates of granule neurons nucleofected with the pmMKO.1/JIP3i or control pmMKO.1 RNAi plasmid were immunoblotted using the JIP3 and AKT antibodies, the latter serving as a loading control. ***H***, Quantification of axon branching of granule neurons transfected with the pmMKO.1/JIP3i or control pmMKO.1 RNAi plasmid together with the GFP expression plasmid, analyzed as in ***B***. Knockdown of JIP3 with this second hairpin increased the number of axonal tips per hundred micrometers (*t* test, $p < 0.001$) and the number of axonal self-contact points per hundred micrometers (*t* test, $p < 0.001$). A total of 156 neurons were measured.

axons that lacked branch points beyond the initial bifurcation of the parallel fibers (Fig. 2*B*). In contrast, granule neuron axons in JIP3 knockdown slices displayed ectopic axon branches (Fig. 2*B*). Quantification of these results revealed an approximately fourfold increase in the percentage of granule neuron axons bearing ectopic branches in JIP3 knockdown cerebellar slices compared with control U6-transfected slices (Fig. 2*C*). These results suggest that JIP3 suppresses axon branching in the cerebellar cortex.

We next determined the role of JIP3 in axon morphogenesis in the rat cerebellum *in vivo*. Using an *in vivo* electroporation method (Fig. 2*D*) (Konishi et al., 2004), we introduced a U6/JIP3i RNAi plasmid that also encodes GFP (U6/JIP3i–cmvGFP) or the corresponding control plasmid (U6–cmvGFP) into P3 rat pups. Animals were killed 5 d after electroporation, at P8. Cerebellar sections were subjected to immunohistochemistry using the GFP antibody and also labeled with the DNA dye bisbenzimide (Hoechst 33258). A clear delineation of the EGL, ML, and IGL was observed in the cerebellar sections (Fig. 2*D*). GFP-positive granule neuron somata were found in the IGL and possessed the characteristic T-shaped parallel fiber axons in the ML (Fig. 2*D*). Examination of the GFP-positive axons in the ML revealed that JIP3 knockdown triggered the formation of ectopic branches in parallel fibers (Fig. 2*E*). Although the majority of parallel fiber axons in control animals had few protrusions as they coursed through the ML, parallel fiber axons in JIP3 knockdown animals displayed frequent ectopic branches (Fig. 2*E*). Quantification of these results revealed an approximately sevenfold increase of the number of ectopic parallel fiber branches in JIP3 knockdown animals compared with control animals (Fig. 2*F*). These results demonstrate that JIP3 acts cell autonomously to suppress axon branching in the mammalian brain *in vivo*.

## GSK3$\beta$ mediates JIP3 restriction of axon branching

The identification of a function for JIP3 in the control of axon branching morphogenesis led us to ask how JIP3 suppresses the formation of axon branches. The JIP3-associated protein kinases JNKs and focal adhesion kinase (FAK) have reported roles in axon growth (Ito et al., 1999; Kelkar et al., 2000; Takino et al., 2002; Chang et al., 2003; Rico et al., 2004; Oliva et al., 2006). Surprisingly, we found that

knockdown of JNKs or FAK failed to induce axon branching in granule neurons (Fig. 3*A–F*). These data suggest that JIP3 suppresses axon branching independently of JNKs and FAK.

The protein kinase GSK3$\beta$ has been implicated in the control of axon branching in mammalian neurons (Kim et al., 2006; Zhao et al., 2009). We therefore asked whether GSK3$\beta$ might mediate the ability of JIP3 to inhibit axon branching. We first characterized the expression pattern of GSK3$\beta$ in primary granule neurons. Both GFP–GSK3$\beta$ and endogenous GSK3$\beta$ were expressed throughout the cytoplasm, including the axon (supplemental Fig. S1*C*,*D*, available at www.jneurosci.org as supplemental material). Consistent with a role for GSK3$\beta$ in JIP3 control of axon branching, we found that GSK3$\beta$ protein levels were diminished in granule neurons during JIP3 knockdown (Fig. 4*A*). Interestingly, JIP3 knockdown had little or no effect on the abundance of GSK3$\alpha$ (Fig. 4*A*), suggesting that JIP3 specifically controls the abundance of GSK3$\beta$ in neurons.

We next investigated the mechanism by which JIP3 controls the abundance of GSK3$\beta$ in neurons. We first tested whether JIP3 knockdown induces the proteasome-dependent degradation of GSK3$\beta$ in neurons. Incubation of granule neurons with the proteasome inhibitor MG132 failed to restore the levels of GSK3$\beta$ in neurons during JIP3 knockdown (supplemental Fig. S4, available at www.jneurosci.org as supplemental material). These results suggest that JIP3 does not appear to stabilize GSK3$\beta$ protein in neurons. We next assessed the role of JIP3 in the regulation of GSK3$\beta$ gene expression. We found that JIP3 knockdown significantly reduced GSK3$\beta$ mRNA levels in neurons, as monitored by real-time RT-PCR analyses (Fig. 4*B*). Together, these results suggest that JIP3 stimulates GSK3$\beta$ gene expression in neurons.

To characterize the role of GSK3$\beta$ in JIP3 control of axon branching morphogenesis, we first assessed the effect of GSK3$\beta$ knockdown on axon morphology of granule neurons. Expression of two shRNAs targeting distinct regions of GSK3$\beta$ (U6/GSK3$\beta$i1 and U6/GSK3$\beta$i2) induced specific knockdown of endogenous GSK3$\beta$ but not GSK3$\alpha$ in granule neurons (Fig. 4*C*). In morphology assays, GSK3$\beta$ knockdown induced exuberant axon branching in granule neurons (Fig. 4*D*). GSK3$\beta$ knockdown substantially increased both the number of axon branch tips and axon self-contact points in neurons (Fig. 4*E*). These data suggest that GSK3$\beta$ knockdown phenocopies the effect of JIP3 knockdown on axon branch morphogenesis.

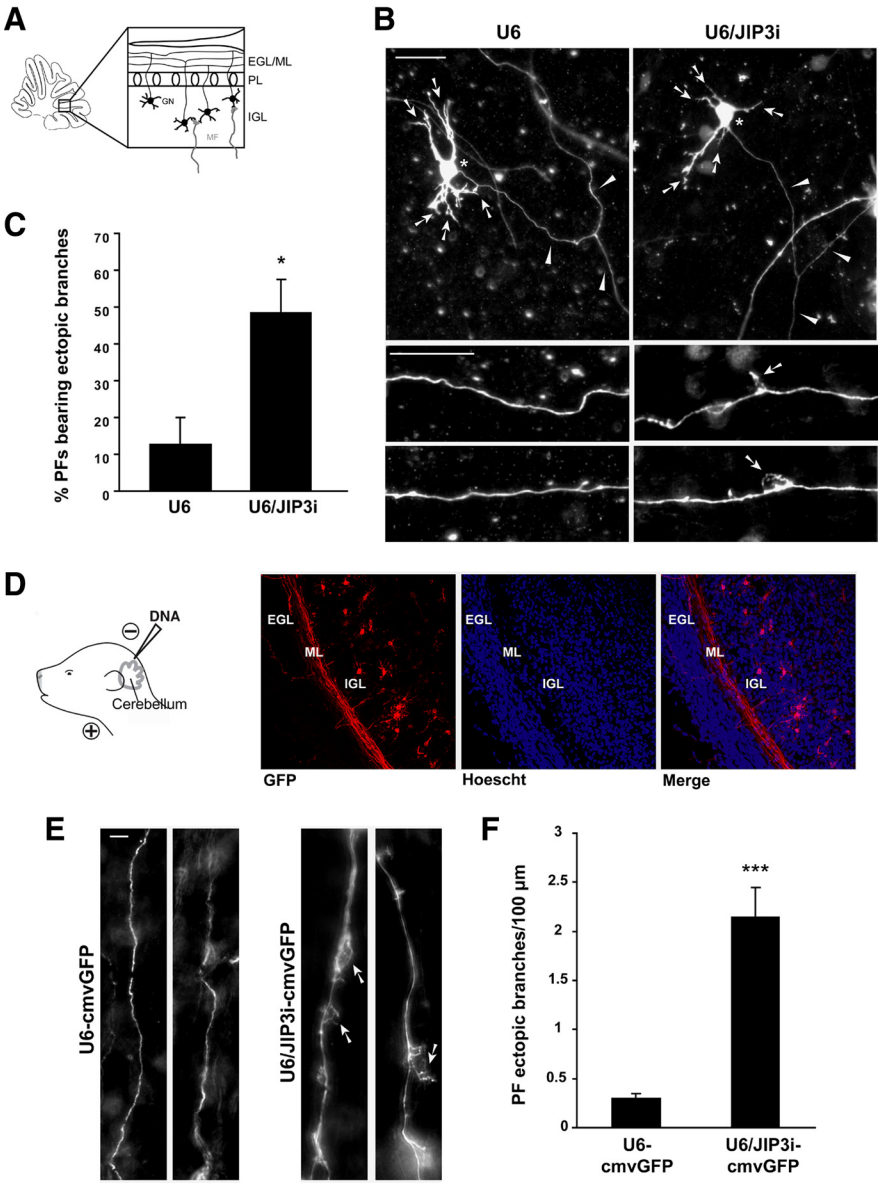


**Figure 2.** JIP3 suppresses axon branching in the cerebellar cortex *in vivo*. ***A***, Schematic of cerebellar slice depicting organization of the cerebellar cortex, including the external granule layer/molecular layer (EGL/ML), the Purkinje cell layer (PL), and the internal granule layer (IGL). ***B***, P9 rat cerebellar slices were transfected at DIV4 with the U6/JIP3i or control U6 RNAi plasmid together with the GFP expression plasmid, fixed 4 d later at DIV8, and subjected to immunohistochemistry using the GFP antibody. Top panels show examples of transfected granule neurons in each condition. Arrows indicate dendrites, asterisks the soma, and arrowheads the parallel fiber axon. Bottom panels show high-magnification images of distal axons in each condition. Arrows in bottom panels point to ectopic branches observed upon JIP3 knockdown. Scale bars, 25 $\mu$m. ***C***, Quantification of slices treated as in ***B***. JIP3 knockdown significantly increased the percentage of parallel fibers bearing one or more ectopic branches (*t* test, $p < 0.05$; $n = 3$). ***D***, Left, Schematic of *in vivo* electroporation paradigm. Briefly, P3 rat pups were injected with DNA at the outer layer of the cerebellum and electroporated. Five days after electroporation, pups were killed and coronal cerebellar sections were subjected to immunohistochemistry using the GFP antibody. Right, Panels show a control section, with the EGL, ML, and IGL identified by Hoechst staining of nuclei. Overlay of GFP staining and Hoechst reveals that the majority of electroporated neurons reside in the IGL and extend axonal processes through the ML. ***E***, High-magnification views of individual GFP-positive parallel fibers in the ML of U6 – cmvGFP- or U6/JIP3i– cmvGFP-electroporated cerebella. Arrows indicate ectopic branches from the primary axonal fiber. Scale bar, 5 $\mu$m. ***F***, Quantification of parallel fiber ectopic branches in the cerebellar cortex in control and JIP3 knockdown animals. The number of ectopic branches in parallel fibers was significantly increased in JIP3 knockdown animals compared with control animals (*t* test, $p < 0.001$). Measurements were collected from a total of 11 animals.

To further compare the effect of inhibition of JIP3 or GSK3$\beta$ on axon branching, we performed time-lapse analyses of JIP3 knockdown and GSK3$\beta$ knockdown neurons. Primary granule neurons transfected with the U6/JIP3i, U6/GSK3$\beta$i2, or control U6 plasmid were imaged at 15 min intervals for a 2 d period

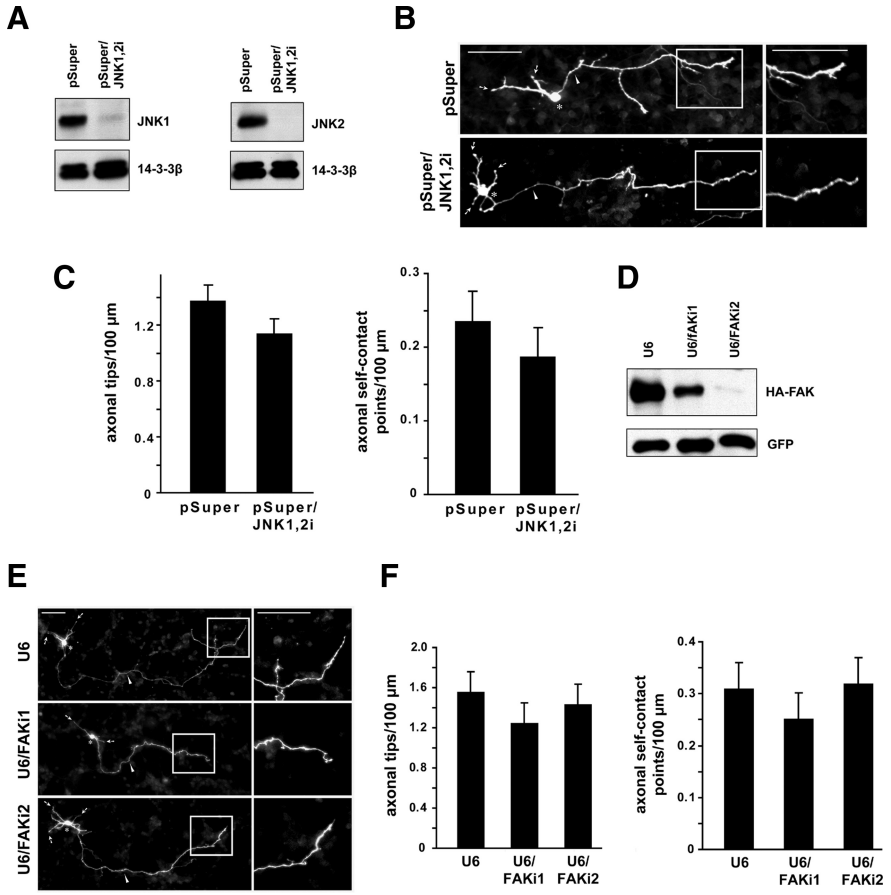


**Figure 3.** JNK knockdown or FAK knockdown do not appear to induce axon branching or self-contact. ***A***, Left, Lysates of HEK293T cells transfected with the FLAG–JNK1 expression plasmid and the pSuper/JNK1,2i or control pSuper RNAi plasmid were immunoblotted using the FLAG and 14-3-3$\beta$ antibodies. Right, Lysates of HEK293T cells transfected with the FLAG–JNK2 expression plasmid and the pSuper/JNK1,2i or control pSuper RNAi plasmid were immunoblotted using the FLAG and 14-3-3$\beta$ antibodies. ***B***, Granule neurons transfected with the pSuper/JNK1,2i or control pSuper RNAi plasmid together with the GFP expression plasmid were analyzed as in Figure 1*B*. Scale bars, 50 $\mu$m. ***C***, Quantification of axon branching of granule neurons treated as in ***B***. JNK knockdown did not significantly alter either the number of axonal tips or the number of axonal self-contact points per hundred micrometers. A total of 149 neurons were measured. ***D***, Lysates of HEK293T cells transfected with the HA–FAK expression plasmid and the U6/FAKi1, U6/FAKi2, or control U6 RNAi plasmid were immunoblotted using the HA and GFP antibodies. ***E***, Granule neurons transfected with the U6/FAKi1, U6/FAKi2, or control U6 plasmid together with the GFP expression plasmid were analyzed as in Figure 1*B*. Scale bars, 50 $\mu$m. ***F***, Quantification of axon branching of granule neurons treated as in ***E***. FAK knockdown with either hairpin did not significantly alter the number of axonal tips or the number of axonal self-contact points per hundred micrometers. A total of 232 neurons were measured.

beginning 24 h after transfection. The temporal analysis of axon morphogenesis allowed the assessment of the type of branching induced by JIP3 knockdown and GSK3$\beta$ knockdown. Two modes of axon branching have been described (Acebes and Ferrús, 2000). In the first mode, the primary growth cone splits into two smaller growth cones, which then grow apart. In the second mode, a branch emerges from the neurite shaft after the primary growth cone has grown past the branch site. The latter mode of branching has been coined "backbranching" (Harris et al., 1987). We observed that the majority of axon branches in primary granule neurons were generated via backbranching (supplemental Fig. S5*A*,*B*, available at www.jneurosci.org as supplemental material). Importantly, we found little or no difference in the percentage of branches formed by backbranching in JIP3 knockdown, GSK3$\beta$ knockdown, or control U6-transfected neurons (supplemental Fig. S5*A*,*B*, available at www.jneurosci.org as supplemental material). These data further corroborate the conclusion that GSK3$\beta$ knockdown phenocopies the effect of JIP3 knockdown on axon branching.

We next tested whether concurrent inhibition of JIP3 and GSK3$\beta$ in granule neurons produces an additive effect on axon branching. We found that simultaneous knockdown of JIP3 and GSK3$\beta$ did not lead to an additive effect on axon branching. Accordingly, the number of axon branch tips and self-contact points in neurons in which both JIP3 and GSK3$\beta$ were knocked down were indistinguishable from those in JIP3 or GSK3$\beta$ knockdown (Fig. 4*F*). These data support a model whereby JIP3 and GSK3$\beta$ may act in a shared pathway to regulate axon branching and self-contact.

### DCX is a novel substrate of GSK3$\beta$ in neurons

We next determined the mechanism by which GSK3$\beta$ regulates axon branching and self-contact in neurons. Because GSK3$\beta$ is a protein kinase, we sought to identify the substrate of GSK3$\beta$ that mediates its ability to suppress axon branching and self-contact. We reasoned that a physiologically relevant substrate of GSK3$\beta$ should harbor conserved putative sites of GSK3 phosphorylation and should be intimately linked to the regulation of microtubule dynamics and the control of branching. The neuronal microtubule-associated protein DCX fulfills both criteria. DCX is enriched in the growth cone and suppresses neurite branching (Gdalyahu et al., 2004; Schaar et al., 2004; Kappeler et al., 2006; Friocourt et al., 2007). Consistent with these observations, endogenous DCX was enriched in the distal portion of the axon compared with the proximal portion of the axon in granule neurons (supplemental Fig. S1*E*, available at www.jneurosci.org as supplemental material). In addition, DCX has a conserved putative site of GSK3$\beta$ phosphorylation at Ser327 (Fig. 5*B*). We therefore asked whether GSK3$\beta$ catalyzes the phosphorylation of DCX and thereby regulates axon branching morphogenesis.

To assess the ability of GSK3 to phosphorylate DCX, we performed an *in vitro* kinase assay using purified recombinant GSK3$\beta$, recombinant DCX protein, and radiolabeled [$\gamma$-$^{32}$P]ATP, the latter to detect the phosphorylation of DCX. Because GSK3$\beta$ phosphorylates substrates that are primed by another phosphorylation event, we determined the ability of GSK3$\beta$ to phosphorylate DCX that was already subjected to a priming *in vitro* kinase reaction. Because the protein kinase JNK phosphorylates and regulates DCX (Gdalyahu et al., 2004) and because JNK can serve as the priming kinase for other GSK3$\beta$ substrates (Sharfi and Eldar-Finkelman, 2008; Morel et al., 2009), we used JNK as the priming kinase in our assays. Recombinant DCX was subjected to an *in vitro* kinase assay using immunoprecipitated JNK1 and nonradiolabeled ATP before the *in vitro* kinase assay with recombinant GSK3$\beta$. We found that GSK3$\beta$ robustly phosphorylated DCX primed with JNK (Fig. 5*A*). Importantly, GSK3$\beta$ failed to induce

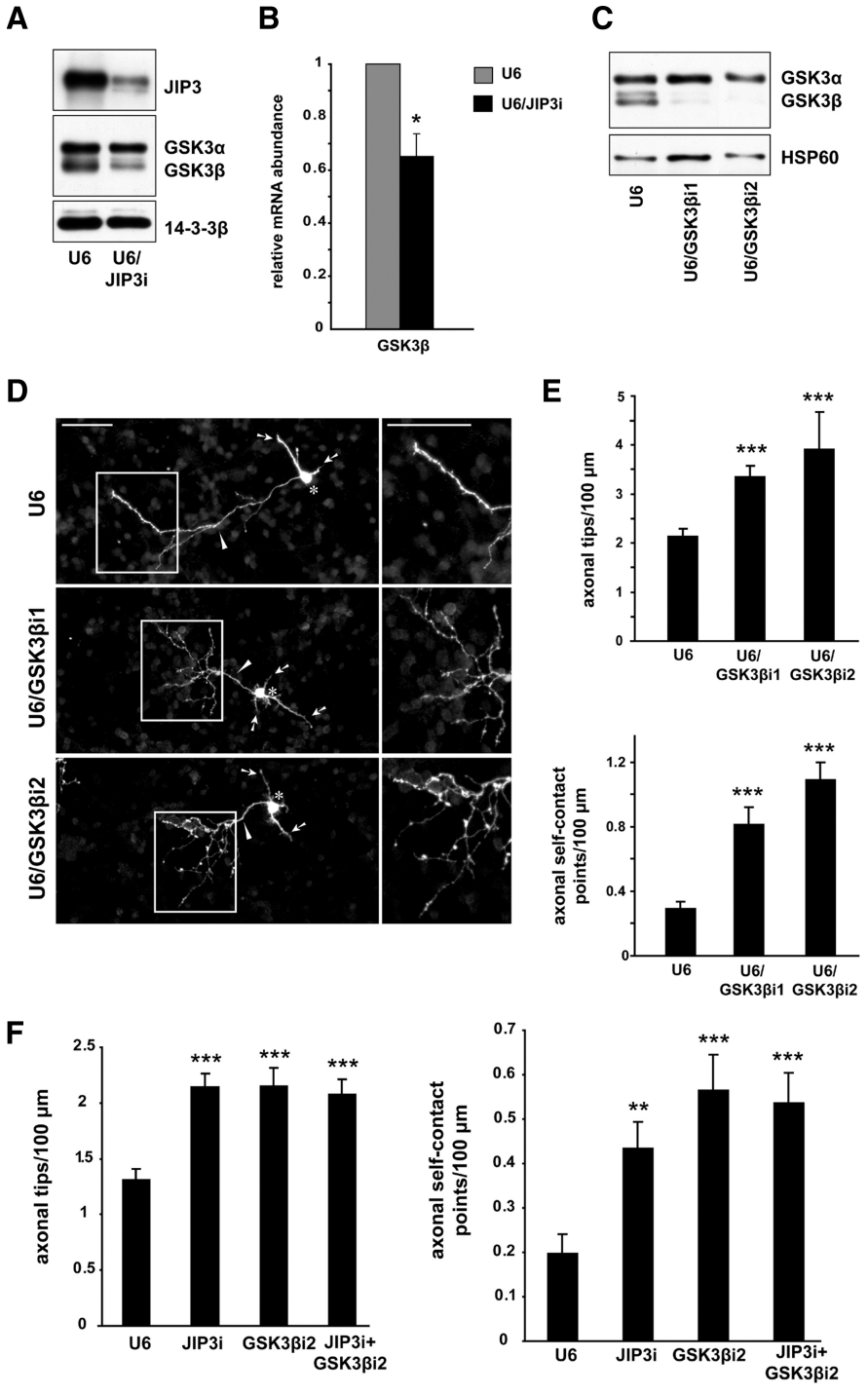


**Figure 4.** GSK3$\beta$ mediates JIP3 restriction of axon branching. ***A***, Lysates of granule neurons nucleofected with the U6/JIP3i or control U6 RNAi plasmid were immunoblotted with the JIP3 and GSK3 antibodies. 14-3-3$\beta$ served as the loading control. Knockdown of JIP3 reduced the levels of GSK3$\beta$ but not GSK3$\alpha$ in neurons. ***B***, RT-PCR was performed to quantify the relative mRNA abundance of GSK3$\beta$ in granule neurons nucleofected with the U6/JIP3i or control U6 RNAi plasmid. Relative mRNA abundance was calculated for the U6/JIP3i condition relative to the U6 condition, normalized by GAPDH. Knockdown of JIP3 significantly decreased the relative levels of GSK3$\beta$ mRNA (*t* test, $p < 0.05$). ***C***, Lysates of granule neurons nucleofected with the U6/GSK3$\beta$i1, U6/GSK3$\beta$i2, or control U6 RNAi plasmid were immunoblotted with the GSK3 and HSP60 antibodies. GSK3$\beta$ RNAi induced knockdown of GSK3$\beta$ but not GSK3$\alpha$ in neurons. ***D***, Granule neurons transfected with the U6/GSK3$\beta$i1, U6/GSK3$\beta$i2, or control U6 RNAi plasmid together with the GFP expression plasmid were analyzed as in Figure 1*B*. Scale bars, 50 $\mu$m. GSK3$\beta$ knockdown triggered the formation of exuberant axon branches. ***E***, Quantification of axon branching of granule neurons treated as in ***D***. For either hairpin, the number of axonal tips and the number of axonal self-contact points per hundred micrometers were both significantly increased in GSK3$\beta$ knockdown neurons compared with control U6-transfected neurons (ANOVA followed by Fisher's PLSD test, $p < 0.001$ for all). A total of 257 neurons were measured. ***F***, Granule neurons transfected with the U6/JIP3i, U6/GSK3$\beta$i2, or both RNAi plasmids or the control U6 RNAi plasmid together with the GFP expression plasmid were analyzed as in Figure 1*B*. Knockdown of either JIP3 or GSK3$\beta$ alone significantly increased the number of axonal tips and the number of axonal self-contact points per hundred micrometers (ANOVA followed by Fisher's PLSD test, $p < 0.01$ or $p < 0.001$ as specified by asterisks). Knockdown of JIP3 and GSK3$\beta$ together did not increase the number of axonal tips or self-contact points compared with knockdown of JIP3 or GSK3$\beta$ alone. A total of 273 neurons were measured.

the phosphorylation of DCX primed with kinase-inactive JNK1 (Fig. 5*A*). Because the priming reaction was performed with nonradiolabeled ATP and JNK1 was washed away from the substrate under high-salt conditions, all $^{32}$P incorporation observed on the autoradiogram is derived from the GSK3$\beta$ reaction. Consistent with this interpretation, DCX primed with JNK1 did not show $^{32}$P incorporation in the absence of GSK3$\beta$ (Fig. 5*A*). In addition, immunoblotting analyses of samples after high-salt washes confirmed the successful deletion of JNK1 (supplemental Fig. S6, available at www.jneurosci.org as supplemental material). Together, these results demonstrate that GSK3$\beta$ phosphorylates DCX *in vitro* and that DCX represents a novel primed substrate of GSK3$\beta$.

Remarkably, the putative GSK3$\beta$ site of phosphorylation, Ser327, in DCX lies four amino acids N-terminal to Ser331, which is an established site of JNK-induced phosphorylation (Fig. 5*B*) (Gdalyahu et al., 2004). In the *in vitro* kinase assays, we found that mutation of Ser327 in recombinant DCX reduced substantially the ability of recombinant GSK3$\beta$ to phosphorylate DCX primed with JNK (Fig. 5*C*). These results reveal that Ser327 represents a major site of GSK3$\beta$-induced phosphorylation of DCX *in vitro*.

We next measured the ability of GSK3$\beta$ to phosphorylate DCX in cells. We found that expression of GSK3$\beta$ induced the phosphorylation of coexpressed DCX in HEK293T cells, as monitored by a mobility shift in DCX (Fig. 5*D*). Expression of a kinase-inactive mutant of GSK3$\beta$, in which the ATP binding site Lys85 is replaced with Ala, failed to induce the phosphorylation of DCX in cells (Fig. 5*D*). Importantly, GSK3$\beta$ failed to induce the phosphorylation of the DCX S327A mutant protein in cells, as reflected by the absence of the mobility shift of DCX S327A during coexpression with GSK3$\beta$ (Fig. 5*E*). We also used a phospho-DCX antibody, which was raised to recognize DCX that is phosphorylated at Ser327 or Thr321, to independently assess the ability of GSK3$\beta$ to phosphorylate DCX in cells. Immunoblotting analyses using phospho-DCX antibody revealed that GSK3$\beta$ induced the phosphorylation of

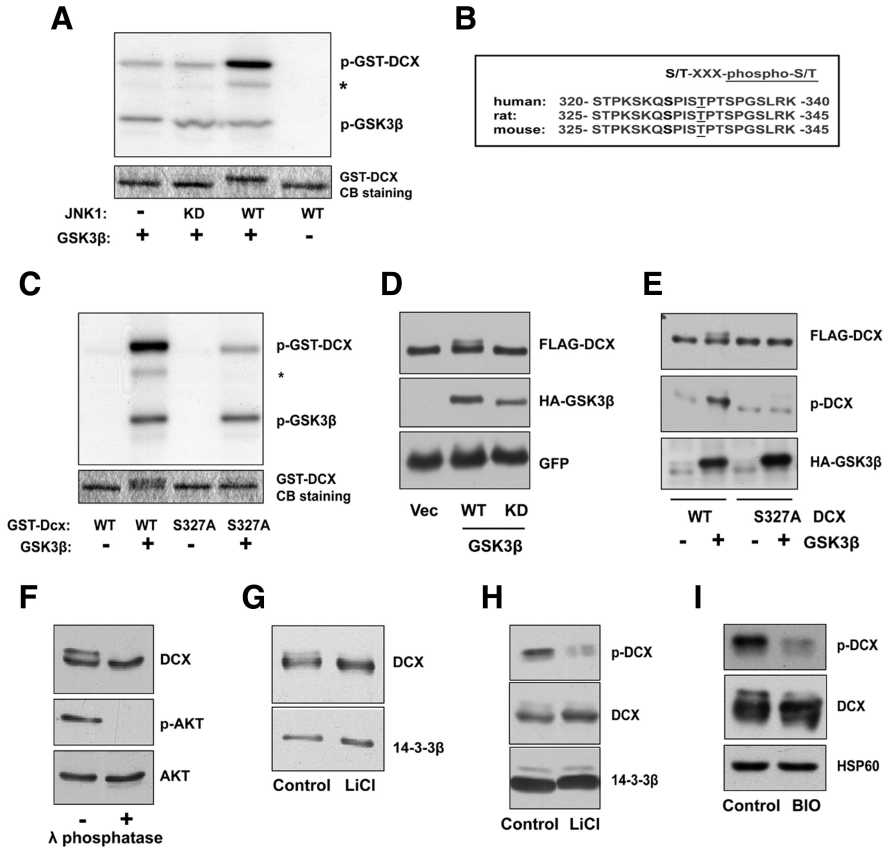


**Figure 5.** GSK3$\beta$ phosphorylates DCX at Ser327. ***A***, Sequential *in vitro* kinase assay. Bacterially purified GST–DCX bound to glutathione beads was first primed with wild-type (WT) or kinase dead (KD) FLAG–JNK1 purified from HEK293T cells. After high-salt washes to remove JNK, GST–DCX was subjected to a kinase assay with GSK3$\beta$ and radiolabeled ATP. The top panel shows $^{32}$P incorporation, and the bottom panel shows Coommassie blue staining. Asterisk denotes a likely degradation product of GST–DCX. GSK3$\beta$ robustly phosphorylates DCX *in vitro*. ***B***, Alignment of human, rat, and mouse DCX protein sequences in the vicinity of a candidate GSK3 phosphorylation site corresponding to human DCX Ser327. ***C***, *In vitro* GSK3$\beta$ kinase assay for JNK-primed WT or S327A GST–DCX, performed as in ***A***. The top panel shows $^{32}$P incorporation, and the bottom panel shows Coommassie blue staining. Asterisk denotes a likely degradation product of GST–DCX. ***D***, Lysates of HEK293T cells transfected with the WT HA–GSK3$\beta$, kinase-dead HA–GSK3$\beta$, or control vector and FLAG–DCX expression plasmids together with the GFP expression plasmid were immunoblotted using the FLAG, HA, and GFP antibodies. ***E***, Lysates of HEK293T cells transfected with the WT HA–GSK3$\beta$ or control vector and the WT FLAG–DCX or S327A FLAG–DCX expression plasmids were immunoblotted using the p-DCX, FLAG, and HA antibodies. GSK3$\beta$ induces the phosphorylation of DCX at Ser327 in cells. ***F***, Granule neuron lysates treated with or without lambda phosphatase were immunoblotted using the DCX, phospho-AKT, and AKT antibodies, the last two serving as controls for the phosphatase treatment and loading, respectively. ***G***, Lysates of granule neurons treated for 24 h with 2 mM NaCl (Control) or 2 mM LiCl were immunoblotted using the DCX and 14-3-3$\beta$ antibodies. ***H***, Lysates of granule neurons treated for 56 h with 2 mM NaCl (Control) or 2 mM LiCl were immunoblotted using the p-DCX and 14-3-3$\beta$ antibodies. Endogenous DCX is phosphorylated at Ser327 in a GSK3$\beta$-dependent manner in neurons. ***I***, Lysates of granule neurons treated for 16 h with 200 nM BIO, a selective inhibitor of GSK3, or the vehicle control DMSO were immunoblotted using the p-DCX, DCX, and HSP60 antibodies. Endogenous DCX is phosphorylated at Ser327 in a GSK3$\beta$-dependent manner in neurons.

wild-type DCX but not the DCX S327A mutant protein in HEK293T cells (Fig. 5*E*). Thus, the GSK3$\beta$-induced phosphorylation signal is Ser327 dependent. Together, these results show that GSK3$\beta$ phosphorylates DCX at Ser327 in cells. In addition, these results show that the phospho-DCX antibody recognizes Ser327-phosphorylated DCX.

We next determined the importance of endogenous GSK3$\beta$ in mediating the phosphorylation of DCX at Ser327 in neurons. First, immunoblotting analyses of lysates of granule neurons using the DCX antibody revealed that endogenous DCX is phosphorylated in granule neurons, as reflected by a mobility shift that is sensitive to treatment of lysates with λ-phosphatase (Fig. 5*F*). Incubation of granule neurons with the GSK3 inhibitor lithium chloride (LiCl) dramatically reduced the phosphorylation of DCX in neurons, as observed by immunoblotting with the DCX antibody (Fig. 5*G*). Using the phospho-DCX antibody, we found that inhibition of GSK3 by LiCl also robustly reduced the phosphorylation of DCX at Ser327 (Fig. 5*H*). Likewise, incubation of granule neurons with the selective GSK3 inhibitor BIO dramatically reduced the phosphorylation of DCX in neurons, as determined by immunoblotting with the DCX antibody or phospho-DCX antibody (Fig. 5*I*). These results suggest that endogenous GSK3$\beta$ induces the phosphorylation of DCX at Ser327 in neurons. Collectively, our experiments *in vitro*, in heterologous cells, and in neurons demonstrate that DCX is a novel bona fide substrate of GSK3$\beta$.

### GSK3$\beta$/DCX signaling restricts axon branching

Having established DCX as a substrate of GSK3$\beta$, we next ascertained the role of the GSK3$\beta$/DCX signaling link in the control of axon branch morphogenesis in neurons. We first tested the effect of DCX knockdown on axon branch morphology in granule neurons. Expression of DCX shRNAs (psiStrike/DCXi) reduced the levels of endogenous DCX in granule neurons (Fig. 6*A*). In morphology assays, we found that DCX knockdown triggered excessive branching of axons compared with neurons transfected with the control psiStrike/Ctrl RNAi plasmid (Fig. 6*B*). Quantification revealed that DCX knockdown led to a greater than twofold increase in both the number of axon tips and self-contact points in neurons (Fig. 6*C*). These results suggest that DCX knockdown phenocopies the effect of JIP3 knockdown and GSK3$\beta$ knockdown on axon branch morphology in neurons. Thus, DCX may operate in a shared pathway with JIP3 and GSK3$\beta$ to suppress axon branching and self-contact in neurons. In agreement with this conclusion, simultaneous knockdown of DCX with JIP3 knockdown or GSK3$\beta$ knockdown did not have an additive effect on axon branching (Fig. 6*D*,*E*). In addition, overexpression of DCX suppressed the JIP3 knockdown- and GSK3$\beta$ knockdown-induced axon branching and self-contact phenotypes (supplemental Fig. S7*A–D*, available at www.jneurosci.org as supplemental material). Together, these data suggest that DCX operates downstream of GSK3$\beta$ in the control of axon branching morphogenesis.

We next determined whether the GSK3$\beta$-induced phosphorylation of DCX at Ser327 regulates axon branching and self-contact. Because the DCX shRNAs target the 3′ untranslated region of DCX, we used DCX encoded by wild-type cDNA to rescue the DCX RNAi-induced phenotype (Bai et al., 2003; Friocourt et al., 2007). Expression of WT DCX–IRES–GFP significantly diminished the DCX RNAi-induced increase in axon

tips and self-contact points (Fig. 6*G*,*H*). These results suggest that the DCX RNAi-induced axon branching and self-contact phenotype is the result of specific knockdown of DCX in neurons and provided us with the means to test the role of phosphorylation of DCX at Ser327 in the ability of DCX to inhibit axon branching and self-contact. We found that S327A DCX–IRES–GFP was not as effective as WT DCX–IRES–GFP in reducing the number of axon tips and self-contact points in granule neurons in the background of DCX RNAi (Fig. 6*G*,*H*). In control experiments, we confirmed that S327A DCX–IRES–GFP and WT DCX–IRES–GFP are expressed at similar levels (Fig. 6*F*). These results suggest that DCX phosphorylation by GSK3$\beta$ at Ser327 contributes to the control of axon branching and self-contact. Collectively, our study shows that a GSK3$\beta$/DCX signaling link regulated by JIP3 controls axon branch morphogenesis in mammalian brain neurons.

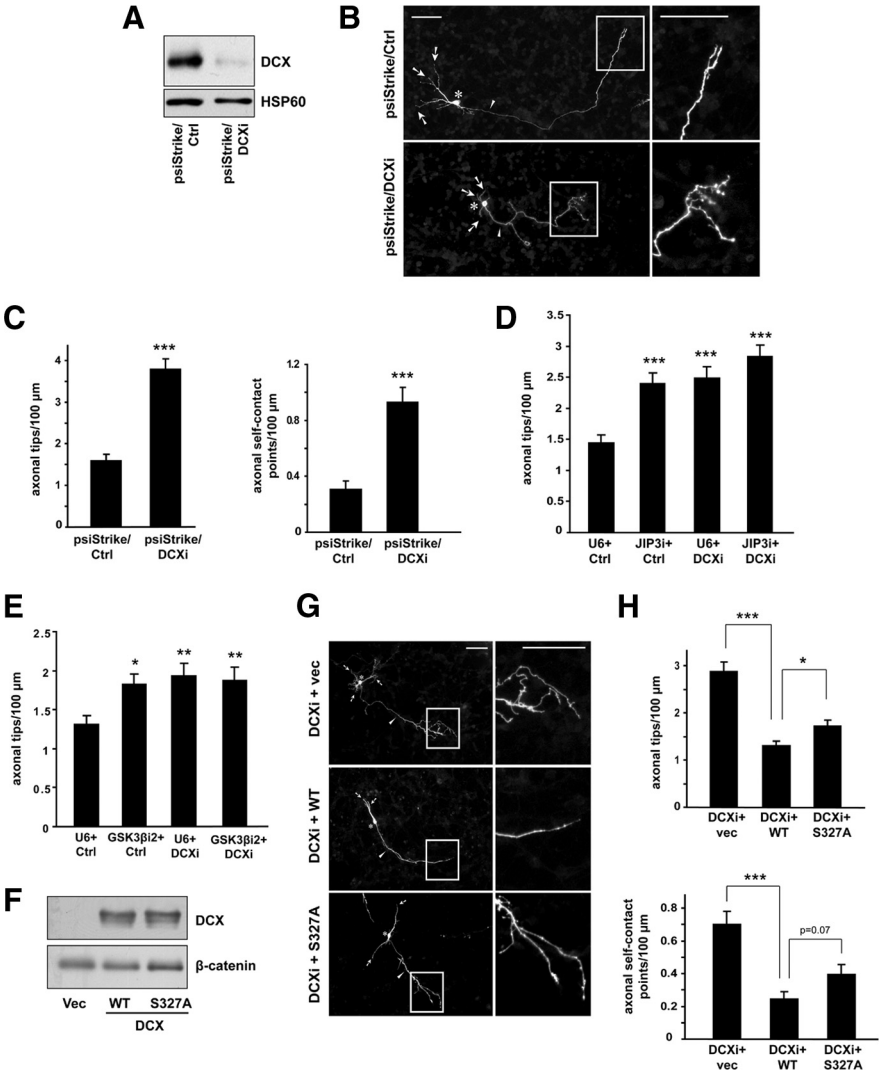


**Figure 6.** GSK3$\beta$/DCX signaling restricts axon branching. ***A***, Lysates of granule neurons nucleofected with the psiStrike/DCXi or psiStrike/Ctrl RNAi plasmid were immunoblotted using the DCX and HSP60 antibodies. ***B***, Granule neurons transfected with the psiStrike/DCXi or psiStrike/Ctrl RNAi plasmid together with the GFP expression plasmid were analyzed as in Figure 1*B*. Scale bars, 50 $\mu$m. DCX knockdown triggered the formation of exuberant axon branches. ***C***, Quantification of axon branching of neurons treated as in ***B***. The number of axonal tips and the number of axonal self-contact points per hundred micrometers were both significantly increased during DCX knockdown (*t* test, $p < 0.001$ for both). A total of 166 neurons were measured. ***D***, Granule neurons transfected with the JIP3 RNAi, DCX RNAi, or both RNAi plasmids or the control RNAi plasmids together with the GFP expression plasmid were analyzed as in Figure 1*B*. Knockdown of either JIP3 or DCX alone significantly increased the number of axonal tips per hundred micrometers (ANOVA followed by Fisher's PLSD test, $p < 0.001$ for both). Knockdown of JIP3 and DCX together did not significantly increase axon branching compared with knockdown of JIP3 or DCX alone. A total of 292 neurons were measured. ***E***, Granule neurons transfected with the GSK3$\beta$ RNAi, DCX RNAi, or both RNAi plasmids or the control RNAi plasmids together with the GFP expression plasmid were analyzed as in Figure 1*B*. Knockdown of either GSK3$\beta$ or DCX alone significantly increased the number of axonal tips per hundred micrometers (ANOVA followed by Fisher's PLSD test, $p < 0.05$ or $p < 0.01$ as specified by asterisks). Knockdown of GSK3$\beta$ and DCX together did not increase axon branching compared with knockdown of GSK3$\beta$ or DCX alone. A total of 264 neurons were measured. ***F***, Lysates of HEK293T cells transfected with the WT DCX–IRES–GFP, S327A DCX–IRES–GFP, or control vector expression plasmid were immunoblotted using the DCX and $\beta$-catenin antibodies, the latter serving as a loading control. ***G***, Granule neurons transfected with the psiStrike/DCXi plasmid together with the WT DCX–IRES–GFP, S327A DCX–IRES–GFP, or control vector expression plasmid were analyzed as in Figure 1*B*. Scale bars, 50 $\mu$m. ***H***, Quantification of axon branching of neurons treated as in ***G***. In the background of DCX knockdown, expression of either WT or S327A DCX–IRES–GFP compared with vector significantly reduced the number of axonal tips and self-contact points per hundred micrometers (ANOVA followed by Fisher's PLSD test, $p < 0.001$ for all). Expression of S327A DCX–IRES–GFP did not reduce axonal tips or self-contacts points as effectively as WT DCX–IRES–GFP in the background of DCX RNAi (ANOVA followed by Fisher's PLSD test, $p < 0.05$ for axonal tips and $p = 0.07$ for axonal self-contact points). A total of 340 neurons were measured.

## Discussion

We have uncovered a novel signaling pathway that cell autonomously controls axon branching morphogenesis in the mammalian brain. There are several major findings in this study. (1) The neuron-enriched signaling protein JIP3 inhibits axon branching and self-contact in granule neurons of the cerebellar cortex. (2) JIP3 restricts branching of granule neuron parallel fiber axons in the cerebellar cortex in cerebellar slices and in postnatal rat pups *in vivo*. (3) JIP3 regulates the expression of the protein kinase GSK3$\beta$ in neurons, which in turn inhibits axon branching and axon self-contact. (4) GSK3$\beta$ phosphorylates the microtubule-associated protein DCX at Ser327 in neurons and thereby inhibits axon branching and self-contact. These findings define a JIP3-regulated GSK3$\beta$/DCX signaling pathway that restrains axon branching and may promote axon self-avoidance.

The identification of the JIP3-regulated GSK3$\beta$/DCX signaling pathway reveals that neurons harbor mechanisms that actively restrict axon branching. Although mechanisms that restrict branches at existing axon terminal arbors or collateral branch sites are beginning to be characterized (Cohen-Cory and Fraser, 1995; Weimann et al., 1999; Livet et al., 2002; Bagri et al., 2003; Homma et al., 2003), mechanisms that actively repress branching in locations in which axons are unbranched remained to be identified. Granule neuron axons branch infrequently. Although all granule neurons have a bifurcated parallel fiber axon, the bifurcation does not represent true branching, because it results from the coordinated fusion of two bipolar axons and the descent of the soma during neuronal migration. Thus, granule neurons provided us with an ideal model system for the study of cell-intrinsic mechanisms that actively suppress axon branching. It will

be interesting in future studies to determine whether components of the JIP3-regulated GSK3β/DCX signaling pathway might also restrict axon branching at terminal arbors or collateral sites.

In addition to enhancing our understanding of axon branching, our findings may provide insight into the molecular regulation of axon self-avoidance. Although the phenomenon of avoidance of axon self-contact has been recognized for some time (Kramer et al., 1985; Wolszon, 1995), the underlying mechanisms have remained to be identified. Our data revealing that JIP3, GSK3β, and DCX inhibit both axon self-contact and axon branching suggest that common mechanisms may have evolved to control these two aspects of axon morphogenesis. Consistent with this idea, the Ig superfamily member DSCAM (Down syndrome cell adhesion molecule) can regulate both axon bifurcation and the divergent segregation of axon branches in *Drosophila* (Wang et al., 2002). A potential explanation for the concurrence of axon self-contact and axon branching during inhibition of the JIP3-regulated GSK3β/DCX pathway that cannot be ruled out is that axon self-contact may occur secondary to increased axon branching.

The finding that JIP3 controls axon branching and self-contact via GSK3β raises the important question of how JIP3 regulates GSK3β in neurons. JIP3 and GSK3β failed to form a physical complex in neurons (data not shown). Consistent with this observation, we have found that JIP3 does not appear to regulate the stability of GSK3β protein. Rather, JIP3 may control GSK3β transcription or mRNA stability. JNK is the only known interacting partner of JIP3 with a clear function in signaling to the nucleus (Johnson and Lapadat, 2002; Bogoyevitch and Kobe, 2006). However, inhibition of JNK failed to mimic JIP3 knockdown in reducing GSK3β levels in neurons (supplemental Fig. S8, available at www.jneurosci.org as supplemental material). Therefore, it will be important in future studies to identify JIP3-dependent signals that regulate GSK3β transcription or mRNA stability.

The identification of DCX as a novel substrate of GSKβ is a key finding in our study. In our analyses, we used the protein kinase JNK as a priming kinase to identify Ser327 as a critical site of GSKβ-induced phosphorylation in DCX. Whether JNK, Cdk5, or a distinct proline-directed protein kinase is the relevant endogenous priming kinase in neurons remains to be determined. Interestingly, phosphorylation of DCX by Cdk5 inhibits the ability of DCX to promote microtubule bundling and suppress axon branching (Tanaka et al., 2004; Bielas et al., 2007). In view of our finding that GSKβ-induced phosphorylation of DCX promotes the function of DCX in the regulation of axon branching and self-contact, these observations raise the possibility that GSK3β-induced phosphorylation might counteract the effects of Cdk5 on DCX function.

Although we focused on Ser327 as a key site of GSK3β-induced phosphorylation in DCX, additional sites of phosphorylation in DCX likely play a role in the GSK3β/DCX signaling link. Mutation of Ser327 reduced substantially but did not abolish the ability of GSK3β to catalyze the phosphorylation of DCX *in vitro*. In addition, mutation of Ser327 impaired but did not block the ability of DCX to suppress axon branching and self-contact in neurons. It will be important in future studies to identify the additional sites of GSK3β-induced phosphorylation in DCX.

Elucidation of the GSK3β/DCX signaling link in our study points to new biological roles for both GSK3β and DCX in the nervous system. Because GSK3β is thought to regulate neurogenesis (Kim et al., 2009; Mao et al., 2009), GSK3β-induced phosphorylation of DCX may contribute to the differentiated state of neurons. Conversely, in view of the established role of DCX in neuronal migration (Bai et al., 2003; Deuel et al., 2006; Friocourt et al., 2007), identification of the GSK3β/DCX signaling link raises the intriguing possibility that GSK3β may promote the migration of neurons in the developing mammalian brain.

DCX mutations are responsible for X-linked lissencephaly in humans, a neurodevelopmental disorder characterized by mental retardation and epilepsy. Abnormalities in neuronal migration play a crucial role in the pathogenesis of X-linked lissencephaly (Allen and Walsh, 1999; Walsh, 1999). The elucidation of the GSK3β/DCX signaling link in the control of axon branching and self-contact raises the important question of whether abnormalities of axon branching and self-contact are featured in the pathology of X-linked lissencephaly. In addition, our findings raise the prospect that deregulation of GSK3β may also contribute to the pathogenesis of neurodevelopmental disorders of cognition and epilepsy.

## References


Acebes A, Ferrús A (2000) Cellular and molecular features of axon collaterals and dendrites. Trends Neurosci 23:557–565.

Akechi M, Ito M, Uemura K, Takamatsu N, Yamashita S, Uchiyama K, Yoshioka K, Shiba T (2001) Expression of JNK cascade scaffold protein JSAP1 in the mouse nervous system. Neurosci Res 39:391–400.

Allen KM, Walsh CA (1999) Genes that regulate neuronal migration in the cerebral cortex. Epilepsy Res 36:143–154.

Altman J, Bayer S (1997) Development of the cerebellar system: in relation to its evolution, structure, and functions. New York: CRC.

Bagri A, Cheng HJ, Yaron A, Pleasure SJ, Tessier-Lavigne M (2003) Stereotyped pruning of long hippocampal axon branches triggered by retraction inducers of the semaphorin family. Cell 113:285–299.

Bai J, Ramos RL, Ackman JB, Thomas AM, Lee RV, LoTurco JJ (2003) RNAi reveals doublecortin is required for radial migration in rat neocortex. Nat Neurosci 6:1277–1283.

Bayarsaikhan M, Takino T, Gantulga D, Sato H, Ito T, Yoshioka K (2007) Regulation of N-cadherin-based cell-cell interaction by JSAP1 scaffold in PC12h cells. Biochem Biophys Res Commun 353:357–362.

Bielas SL, Serneo FF, Chechlacz M, Deerinck TJ, Perkins GA, Allen PB, Ellisman MH, Gleeson JG (2007) Spinophilin facilitates dephosphorylation of doublecortin by PP1 to mediate microtubule bundling at the axonal wrist. Cell 129:579–591.

Bilimoria PM, Bonni A (2008) Cultures of cerebellar granule neurons. Cold Spring Harb Protoc 3:1201–1207.

Bogoyevitch MA, Kobe B (2006) Uses for JNK: the many and varied substrates of the c-Jun N-terminal kinases. Microbiol Mol Biol Rev 70:1061–1095.

Bowman AB, Kamal A, Ritchings BW, Philp AV, McGrail M, Gindhart JG, Goldstein LS (2000) Kinesin-dependent axonal transport is mediated by the Sunday driver (SYD) protein. Cell 103:583–594.

Byrd DT, Kawasaki M, Walcoff M, Hisamoto N, Matsumoto K, Jin Y (2001) UNC-16, a JNK-signaling scaffold protein, regulates vesicle transport in *C. elegans*. Neuron 32:787–800.

Chang L, Jones Y, Ellisman MH, Goldstein LS, Karin M (2003) JNK1 is required for maintenance of neuronal microtubules and controls phosphorylation of microtubule-associated proteins. Dev Cell 4:521–533.

Cohen-Cory S, Fraser SE (1995) Effects of brain-derived neurotrophic factor on optic axon branching and remodelling in vivo. Nature 378:192–196.

Deuel TA, Liu JS, Corbo JC, Yoo SY, Rorke-Adams LB, Walsh CA (2006) Genetic interactions between doublecortin and doublecortin-like kinase in neuronal migration and axon outgrowth. Neuron 49:41–53.

Friocourt G, Liu JS, Antypa M, Rakic S, Walsh CA, Parnavelas JG (2007) Both doublecortin and doublecortin-like kinase play a role in cortical interneuron migration. J Neurosci 27:3875–3883.

Gaudillière B, Shi Y, Bonni A (2002) RNA interference reveals a requirement for myocyte enhancer factor 2A in activity-dependent neuronal survival. J Biol Chem 277:46442–46446.

Gaudillière B, Konishi Y, de la Iglesia N, Yao G, Bonni A (2004) A CaMKII-

NeuroD signaling pathway specifies dendritic morphogenesis. Neuron 41:229–241.

Gdalyahu A, Ghosh I, Levy T, Sapir T, Sapoznik S, Fishler Y, Azoulai D, Reiner O (2004) DCX, a new mediator of the JNK pathway. EMBO J 23:823–832.

Hammond JW, Griffin K, Jih GT, Stuckey J, Verhey KJ (2008) Co-operative versus independent transport of different cargoes by Kinesin-1. Traffic 9:725–741.

Harris WA, Holt CE, Bonhoeffer F (1987) Retinal axons with and without their somata, growing to and arborizing in the tectum of *Xenopus* embryos: a time-lapse video study of single fibres in vivo. Development 101:123–133.

Hatten ME (1999) Central nervous system neuronal migration. Annu Rev Neurosci 22:511–539.

Homma N, Takei Y, Tanaka Y, Nakata T, Terada S, Kikkawa M, Noda Y, Hirokawa N (2003) Kinesin superfamily protein 2A (KIF2A) functions in suppression of collateral branch extension. Cell 114:229–239.

Ito M, Yoshioka K, Akechi M, Yamashita S, Takamatsu N, Sugiyama K, Hibi M, Nakabeppu Y, Shiba T, Yamamoto KI (1999) JSAP1, a novel jun N-terminal protein kinase (JNK)-binding protein that functions as a scaffold factor in the JNK signaling pathway. Mol Cell Biol 19:7539–7548.

Johnson GL, Lapadat R (2002) Mitogen-activated protein kinase pathways mediated by ERK, JNK, and p38 protein kinases. Science 298:1911–1912.

Kappeler C, Saillour Y, Baudoin JP, Tuy FP, Alvarez C, Houbron C, Gaspar P, Hamard G, Chelly J, Métin C, Francis F (2006) Branching and nucleokinesis defects in migrating interneurons derived from doublecortin knockout mice. Hum Mol Genet 15:1387–1400.

Kelkar N, Gupta S, Dickens M, Davis RJ (2000) Interaction of a mitogen-activated protein kinase signaling module with the neuronal protein JIP3. Mol Cell Biol 20:1030–1043.

Kim WY, Zhou FQ, Zhou J, Yokota Y, Wang YM, Yoshimura T, Kaibuchi K, Woodgett JR, Anton ES, Snider WD (2006) Essential roles for GSK-3s and GSK-3-primed substrates in neurotrophin-induced and hippocampal axon growth. Neuron 52:981–996.

Kim WY, Wang X, Wu Y, Doble BW, Patel S, Woodgett JR, Snider WD (2009) GSK-3 is a master regulator of neural progenitor homeostasis. Nat Neurosci 12:1390–1397.

Konishi Y, Stegmüller J, Matsuda T, Bonni S, Bonni A (2004) Cdh1-APC controls axonal growth and patterning in the mammalian brain. Science 303:1026–1030.

Kornack DR, Giger RJ (2005) Probing microtubule +TIPs: regulation of axon branching. Curr Opin Neurobiol 15:58–66.

Kramer AP, Goldman JR, Stent GS (1985) Developmental arborization of sensory neurons in the leech *Haementeria ghilianii*. I. Origin of natural variations in the branching pattern. J Neurosci 5:759–767.

Livet J, Sigrist M, Stroebel S, De Paola V, Price SR, Henderson CE, Jessell TM, Arber S (2002) ETS gene Pea3 controls the central position and terminal arborization of specific motor neuron pools. Neuron 35:877–892.

Mao Y, Ge X, Frank CL, Madison JM, Koehler AN, Doud MK, Tassa C, Berry EM, Soda T, Singh KK, Biechele T, Petryshen TL, Moon RT, Haggarty SJ, Tsai LH (2009) Disrupted in schizophrenia 1 regulates neuronal progenitor proliferation via modulation of GSK3beta/beta-catenin signaling. Cell 136:1017–1031.

Morel C, Carlson SM, White FM, Davis RJ (2009) Mcl-1 integrates the opposing actions of signaling pathways that mediate survival and apoptosis. Mol Cell Biol 29:3845–3852.

Oliva AA Jr, Atkins CM, Copenagle L, Banker GA (2006) Activated c-Jun N-terminal kinase is required for axon formation. J Neurosci 26:9462–9470.

Ramon y Cajal S (1995) The cerebellum. In: Histology of the nervous system (N. Swanson and L. Swanson, translators). New York: Oxford UP.

Rico B, Beggs HE, Schahin-Reed D, Kimes N, Schmidt A, Reichardt LF (2004) Control of axonal branching and synapse formation by focal adhesion kinase. Nat Neurosci 7:1059–1069.

Sato S, Ito M, Ito T, Yoshioka K (2004) Scaffold protein JSAP1 is transported to growth cones of neurites independent of JNK signaling pathways in PC12h cells. Gene 329:51–60.

Schaar BT, Kinoshita K, McConnell SK (2004) Doublecortin microtubule affinity is regulated by a balance of kinase and phosphatase activity at the leading edge of migrating neurons. Neuron 41:203–213.

Sharfi H, Eldar-Finkelman H (2008) Sequential phosphorylation of insulin receptor substrate-2 by glycogen synthase kinase-3 and c-Jun NH2-terminal kinase plays a role in hepatic insulin signaling. Am J Physiol Endocrinol Metab 294:E307–E315.

Takino T, Yoshioka K, Miyamori H, Yamada KM, Sato H (2002) A scaffold protein in the c-Jun N-terminal kinase signaling pathway is associated with focal adhesion kinase and tyrosine-phosphorylated. Oncogene 21:6488–6497.

Tanaka T, Serneo FF, Tseng HC, Kulkarni AB, Tsai LH, Gleeson JG (2004) Cdk5 phosphorylation of doublecortin ser297 regulates its effect on neuronal migration. Neuron 41:215–227.

Verhey KJ, Meyer D, Deehan R, Blenis J, Schnapp BJ, Rapoport TA, Margolis B (2001) Cargo of kinesin identified as JIP scaffolding proteins and associated signaling molecules. J Cell Biol 152:959–970.

Walsh CA (1999) Genetic malformations of the human cerebral cortex. Neuron 23:19–29.

Wang J, Zugates CT, Liang IH, Lee CH, Lee T (2002) *Drosophila* Dscam is required for divergent segregation of sister branches and suppresses ectopic bifurcation of axons. Neuron 33:559–571.

Weimann JM, Zhang YA, Levin ME, Devine WP, Brûlet P, McConnell SK (1999) Cortical neurons require Otx1 for the refinement of exuberant axonal projections to subcortical targets. Neuron 24:819–831.

Whitmarsh AJ, Davis RJ (1998) Structural organization of MAP-kinase signaling modules by scaffold proteins in yeast and mammals. Trends Biochem Sci 23:481–485.

Wolszon L (1995) Cell-cell interactions define the innervation patterns of central leech neurons during development. J Neurobiol 27:335–352.

Yasuda J, Whitmarsh AJ, Cavanagh J, Sharma M, Davis RJ (1999) The JIP group of mitogen-activated protein kinase scaffold proteins. Mol Cell Biol 19:7245–7254.

Zhao Z, Wang Z, Gu Y, Feil R, Hofmann F, Ma L (2009) Regulate axon branching by the cyclic GMP pathway via inhibition of glycogen synthase kinase 3 in dorsal root ganglion sensory neurons. J Neurosci 29:1350–1360.